4ICEGE Thessaloniki-GREECE 2007

4th International Conference on
Earthquake Geotechnical Engineering
June 25-28, 2007
Paper No. 1225

SEISMIC PERFORMANCE EVALUATION OF POTENTIALLY LIQUEFIABLE EARTH DAMS

Juan M. MAYORAL [1] and Miguel P. ROMO[2]

ABSTRACT

Seismic performance evaluations of earth dams are essential to characterize the geotechnical risk implied by slope stability failures. There are a large number of case histories compiled in the international technical literature, which report failures of these types of earthen structures caused by moderate to large magnitude earthquakes. The observed damage is more important when liquefaction occurs on the dam body and foundation, which often leads to cracking, settlements, tilting, and general distortion of the dam geometry. Analyses based on limit equilibrium are generally sufficient to establish hazard zones. However, numerical models with solution schemes formulated in the time domain, which are capable of taking into account the kinematics of the soil movement more realistically, are needed to quantify the geotechnical risk. This paper describes the application of a practice-oriented simplified constitutive model, which implemented in a lagragian finite difference platform, is capable of predicting the accumulation of pore pressure due to earthquake loading in fine-grained saturated materials, the reduction of shear strength, and its effect on the development of permanent displacements. The model uses a bilinear Mohr-Coulomb type failure criterion coupled with an incremental pore pressure generation scheme. The pore pressure is accumulated as a function of the number of stress cycles. The tangent soil stiffness and hysteretic damping are modified with the loading history. The model capability to evaluate the seismic response of earth dams is illustrated through the analysis of a case history comparing the model predictions with actual field measures. The model is able to properly capture the kinematics of the slope failure and the observed damage. The measured permanent displacements after liquefaction and those computed with the model are in good agreement.

Keywords: Seismic, Liquefaction, Earth dams, Slope failure

INTRODUCTION

Dam seismic stability analyses are a key step in risk evaluations to ensure that catastrophic failures, such as those reported in the technical literature (e.g. Seed et al., 1969 & 1973; Castro et al., 1985; Davis, C.A & Bardet, J. P., 1994), will not occur. In particular, these evaluations become more complex when the dam is built with loose to medium fined-grained, saturated materials. In these cases, the analysis should account for the degree of internal drainage and the characteristics of the design earthquake, to properly estimate the amount of pore pressure built-up during the seismic event, the corresponding impact in the reduction of the shear strength, and the modification of the dynamic properties of the soil (i.e. shear stiffness and damping). Based on these evaluations, proper assessment of the volume of material mobilized during a potential failure and the pattern and speed of deformation can be achieved, providing guidance to estimate the extension of the affected zones. Thus, maps of geotechnical hazard and quantification of specific risks can be constructed.

[1] Associate Professor, Instituto de Ingeniería, Coordinación de Geotecnia, UNAM, México, Email: jmayoralv@iingen.unam.mx

[2] Professor, Instituto de Ingeniería, Coordinación de Geotecnia, UNAM, México, Email: mro@iingen.unam.mx

Pseudo-static methods, based on limit equilibrium, and others formulated considering the sliding block mechanism, are enough to define geotechnical hazard zones but insufficient to quantify the seismic risk, which requires a complete understanding of the kinematics of the slope failure process (Morgenstern, 1985). A complete representation of the failure mechanism usually requires using constitutive models to simulate the dynamic response of the soil, coupled with numerical techniques, such as the finite differences or the finite element. Such models have evolved over time, from the classical hyperbolic Masing-type models (e.g. Finn et al., 1976) to more sophisticated models based on bounding surface hypoplasticity theory (e.g. Wang et al., 2006).

A fully nonlinear dynamic analysis of potentially liquefiable dams requires using a numerical model able to account for the effect of generation and dissipation of pore pressure within the dam body and foundation and its impact in the variation of shear strength, which in turn, will lead to permanent displacements. Probably, the best representation of the liquefaction problem can be achieved with a fully coupled constitutive model, where the equation of motion is solved simultaneously with the diffusion equation during an effective stress analysis (Wang et al., 2006). However, in general, the more sophisticated a constitutive model is, the more cumbersome it becomes to use in engineering practice.

This paper presents a practice-oriented numerical scheme, which implemented in a lagragian platform, appears to capture well the overall behavior of ground response in geotechnical problems in which large deformations are likely to occur, such as liquefaction or cyclic mobility. This approach is an enhancement of the formulation proposed by Dawson et al. (2001). The method allows incorporating the degree of internal distortion of the mobilized soil mass, the drainage conditions, localization of failure planes near to the slope surface, and the plastic yield at depth. The methodology is illustrated through its application to the analysis of a case history, and the model predictions are compared with field measurements, both qualitatively and quantitatively.

ANALYTICAL FRAMEWORK

The problem of soil liquefaction during strong shaking is due to the development of excess pore pressure during cyclic loading, and has been traditionally studied following two approaches: cyclic stresses and cyclic strains. Historically, methodologies based on stress cycles have been the most popular in practice, mainly because they can be estimated directly from an acceleration time history measured or computed in a given soil profile (e.g. Seed e Idriss, 1971), whereas the estimation of strain cycles requires making assumptions regarding the stress-strain relationship of the soil. The cyclic stress approach considers that the liquefaction potential of a soil stratum is a function of the number and magnitude of shear stresses applied to the soil during the dynamic event. The cyclic shear stresses are expressed in terms of the cyclic stress ratio (CSR), defined as the ratio between the cyclic shear stress τ_{cy} acting on the failure plane, divided by the initial vertical effective stress σ'_{vo}.

$$CSR=\tau_{cy}/\sigma'_{vo} \quad (1)$$

This relationship depends mainly on the initial state of stresses existing in the ground and the seismic load, expressed in terms of the number of equivalent cycles, which in turn is defined by the duration, intensity and frequency content of the earthquake.

It is common practice to describe the soil resistance to liquefaction through a curve of cyclic strength, which relates the number of cycles required to have a pore pressure ratio of one, with its corresponding cyclic stress ratio (Figure 1). The pore pressure ratio, r_u, is defined as $r_u= \Delta_{ug}/\sigma_{vo}'$, were Δ_{ug}, is the generated pore pressure. These curves can be obtained from laboratory testing, or derived from CSR plots generated from field measurements and back analysis of case histories. Thus, the cyclic strength of a soil is mainly a function of its relative density, including grain gradation and shape, and fines content.

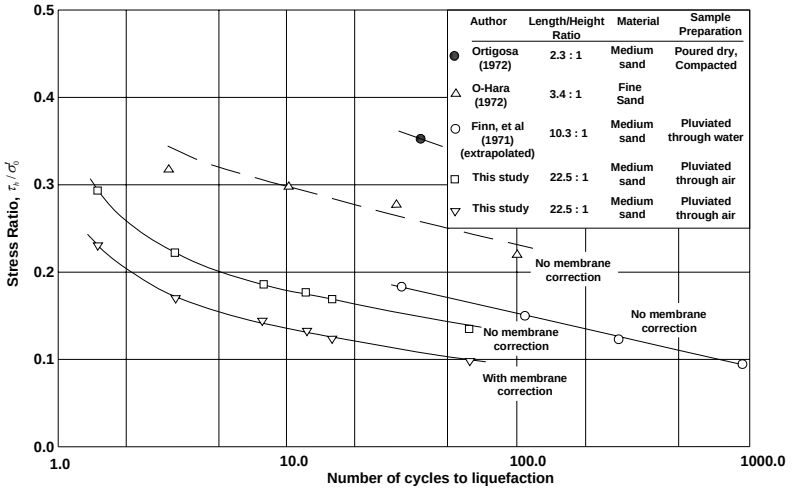

Figure 1. Resistance to liquefaction determined experimentally (Modified from Seed, 1976)

An analysis based on the cyclic stress approach should include at least the following steps:

1) Evaluation of shear stress time histories at each soil layer conducting numerical analyses of wave propagation or soil-structure interaction.
2) Approximation of the shear stress histories to an equivalent number of uniform stress cycles, N_{eq}
3) Comparison of the number of equivalent cycles with the liquefaction resistance curve of the soil to determine if there will be liquefaction, and how close the soil is to the condition r_u=1.
4) Evaluation of the effect that the computed number of equivalent stress cycles has in the soil, in terms of change of volume, and increase of pore pressure.

NUMERICAL SCHEME

The numerical scheme utilized in this work is based on the so-called simplified procedure, proposed by Seed e Idriss (1971) to model liquefaction. Thus, the pore water pressure is incremented directly as a function of the number of uniform cyclic stresses induced in the soil by the earthquake. In turn, this increase in pressure will decrease both the soil stiffness and the shear strength. The shear strength is assumed to follow a modified bilinear Mohr-Coulomb law (Figure 2). In this manner, the soil strength is a function of the relative density of the material, fines content, and residual strength. Even though this type of formulations simplify considerably many aspects of the real soil behavior because it considers that the generation of pore pressure is due directly to the cyclic shear stress instead of a contraction of the soil skeleton, this type of models seems to provide adequate estimations to geotechnical problems where plastic deformations are significant. The validity of similar approaches to predict permanent deformations due to earthquake loading has been demonstrated by Roth et al. (1986) through comparisons with centrifuge test data for dry sands, and by Dawson et al. (2001) for saturated sands, comparing numerical predictions with actual measurements obtained directly from case histories.

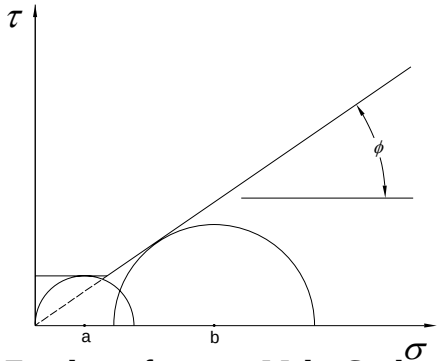

Figure 2. Envelope of stresses Mohr-Coulumb modified

Mechanism of pore pressure generation

The mechanism of pore pressure generation is an enhancement of an existing formulation proposed by Dawson et al. (2001), and is illustrated in Figure 3. The history of horizontal shear stresses is monitored, and each time the shear stress passes twice throughout zero, a semi-cycle of that particular cyclic stress ratio, CSR, obtained as τ_{cy}/σ'_{vo} is accumulated (Figure 3), developing and amount of excess pore pressure, Δ_{ug}. This Δ_{ug}, is described in terms of the pore pressure ratio. Each semi-cycle will generate an increment in pore pressure proportional to the total number of cycles which are necessary to reach the condition $r_u = 1$ for a given CSR. The increment of pore pressure, Δu_{gi}, is computed as $\Delta u_{gi}=\Delta r_{ui}\sigma'_v$. When the pore pressure goes up, the effective stress goes down and in turn the shear strength, and soil stiffness. The tangent soil stiffness is modified using the following expression $G=G_{max}(\sigma'_v/\sigma'_{vo})$, where σ'_v is the current value of vertical effective stress for that semi-cycle. Thus, the secant modulus will decrease not only due to the loss of shear strength, which decreases as a function of σ'_v, but also directly due to changes in the tangent modulus of plastic stress-strain hysteretic loops.

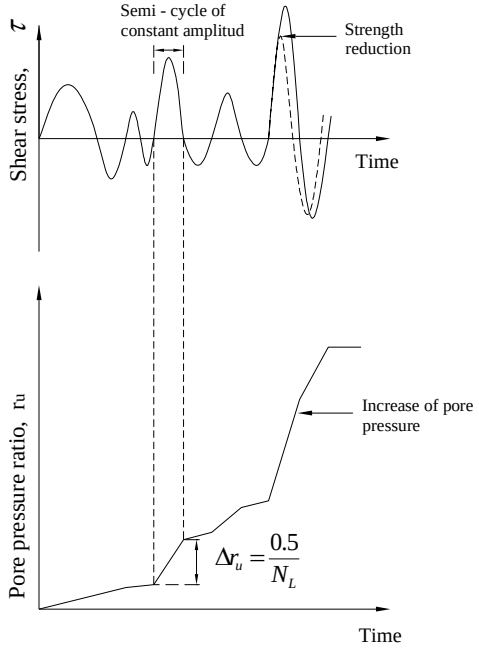

Figure 3. Interdependence of the cyclic shear stress, the pore pressure and the number of cyclic stresses

Residual strength after liquefaction

After liquefaction, the shear strength of the soil is mostly provided by its residual strength, s_r. Thus, s_r, is a key parameter to assess levels of permanent displacements levels and the overall dam stability at the end of the earthquake. The model presented herein incorporates the residual strength using a bilinear failure envelope. This envelope consists of an initial cohesion and a friction value of zero, which extends until it intersects the Mohr-Coulomb envelope (Figure 2). The residual strength can be determined from Standard Penetration test, SPT, corrected blow counts for clean sand $(N_1)_{60\text{-}cs}$ (e.g., Seed and Harder, 1990). The residual strength constitutes the lower bound of the shear strength, and will essentially define the soil resistance when the pore pressure ratio, r_u, becomes 1.

Model Performance

To illustrate the model performance, a parametric study was conducted using three different uniform stress histories, with amplitudes and frequencies varying from 9.81 kPa to 49.03 kPa, and from 0.10 to 0.02 Hz, respectively, as it is shown in Figure 4. The material was assumed as saturated clean sand with a corrected SPT $(N_1)_{60\text{-}cs}$ value of 17, a shear wave velocity of 250 m/s, and a residual strength, s_r, of 33 kPa approximately. The initial vertical stress was 101.3 kPa (i.e. 1 atm), and the initial pore

pressure was assumed to be 20 kPa. As can be noticed, the pore pressure increases linearly each semi-cycle, starting from the initial pore water conditions. For tests 2 and 3, the pore increases until reaches the total vertical stress after 12 seconds approximately, and thus, r_u becomes one. For test 1 no appreciable increase in pore pressure is observed, due to the relative low shear stress amplitude.

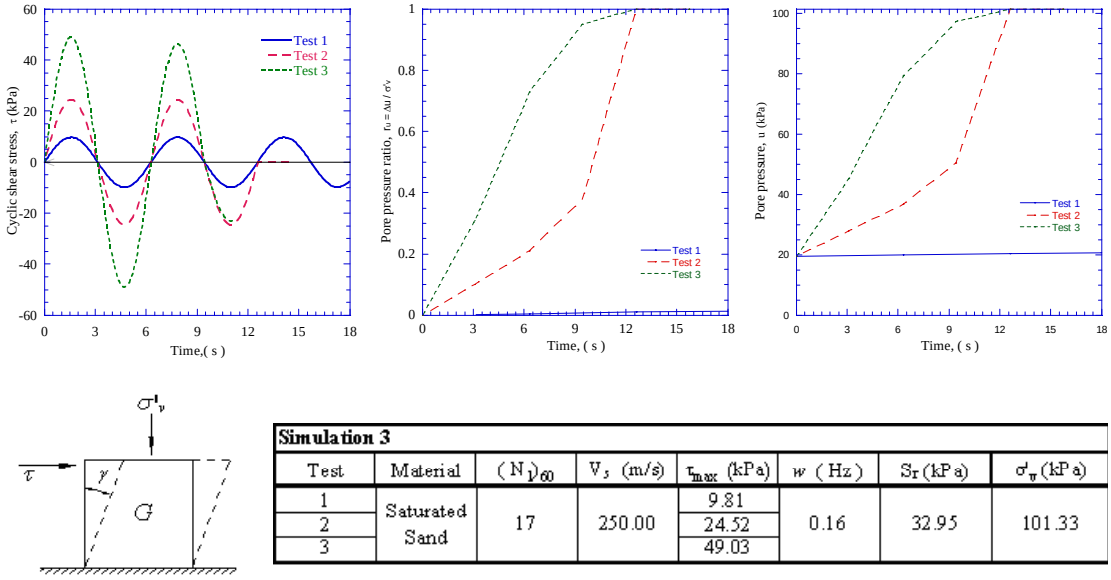

Simulation 3

Test	Material	$(N_1)_{60}$	V_s (m/s)	τ_{max} (kPa)	w (Hz)	S_r (kPa)	σ'_v (kPa)
1	Saturated Sand	17	250.00	9.81	0.16	32.95	101.33
2				24.52			
3				49.03			

Figure 4. Model response for uniform cycles

Similarly, Figure 5 shows the model response for a non uniform stress history. The maximum stress amplitude was about 49 kPa and the mean frequency was 0.16 Hz. The material properties were the same as those considered in the previous case. The initial vertical stress was 101.325 kPa. Again, the initial pore pressure was assumed to be 20 kPa. The material reaches initial liquefaction after 31 seconds approximately.

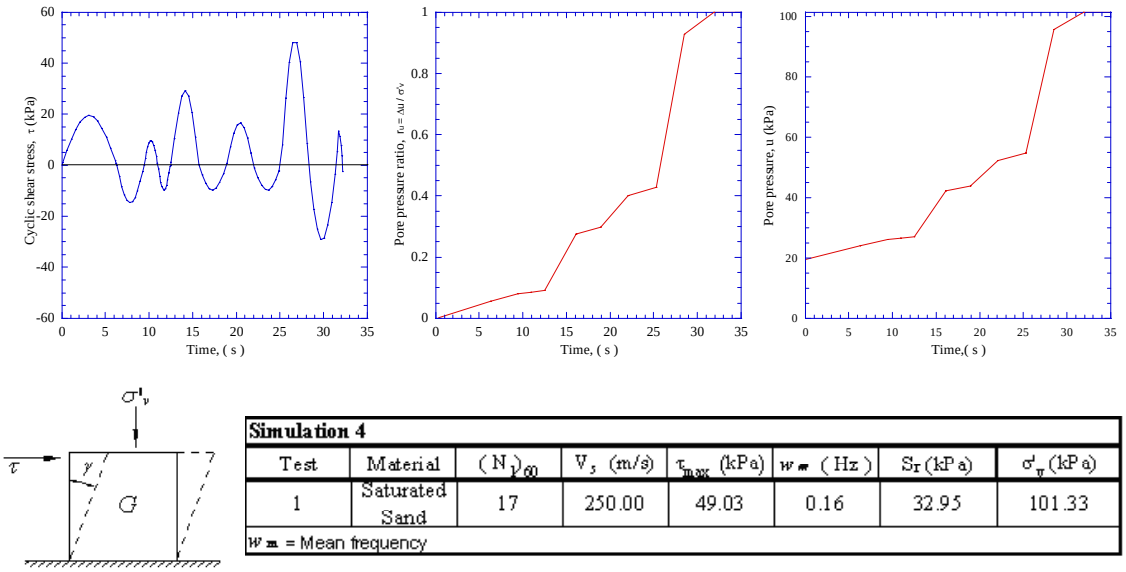

Simulation 4

Test	Material	$(N_1)_{60}$	V_s (m/s)	τ_{max} (kPa)	w_m (Hz)	S_r (kPa)	σ'_v (kPa)
1	Saturated Sand	17	250.00	49.03	0.16	32.95	101.33

w_m = Mean frequency

Figure 5. Model response for irregular cycles

MODEL APLICATION TO THE EVALUATION OF A CASE HYSTORY

The model described above was implemented in a finite difference platform to be used for analyzing the dynamic response of potentially liquefiable earth dams. A case study, which has been analyzed in the past by numerous researchers, the performance of the Lower San Fernando Dam during the Northridge Earthquake, was considered to illustrate the methodology.

Background

Located in Los Angeles County, Lower San Fernando dam, along with Los Angeles and Upper San Fernando dams constitutes the hydraulic complex Van Norman (Figure 6), which controls from 50 to 75% of the total water supply of Los Angeles City (Davis y Bardet, 1994). Due to its strategic importance, its seismic behavior observed during several seismic events have been studied in the past by numerous researches and practitioners (e.g., Dawson, et al., 2001; Bardet y Davis, 1996a y b; Davis y Bardet, 1994; Seed et al., 1973; Seed et al., 1989). During the 1994 Northridge earthquake, the Van Norman Complex was severely shook, leading to generation of sand boils, lateral spreading, settlement and cracking along the complex and in particular in the Upper and Lower San Fernando hydraulic fills dams. Similarly, Los Angeles reservoir underwent measurable movement.

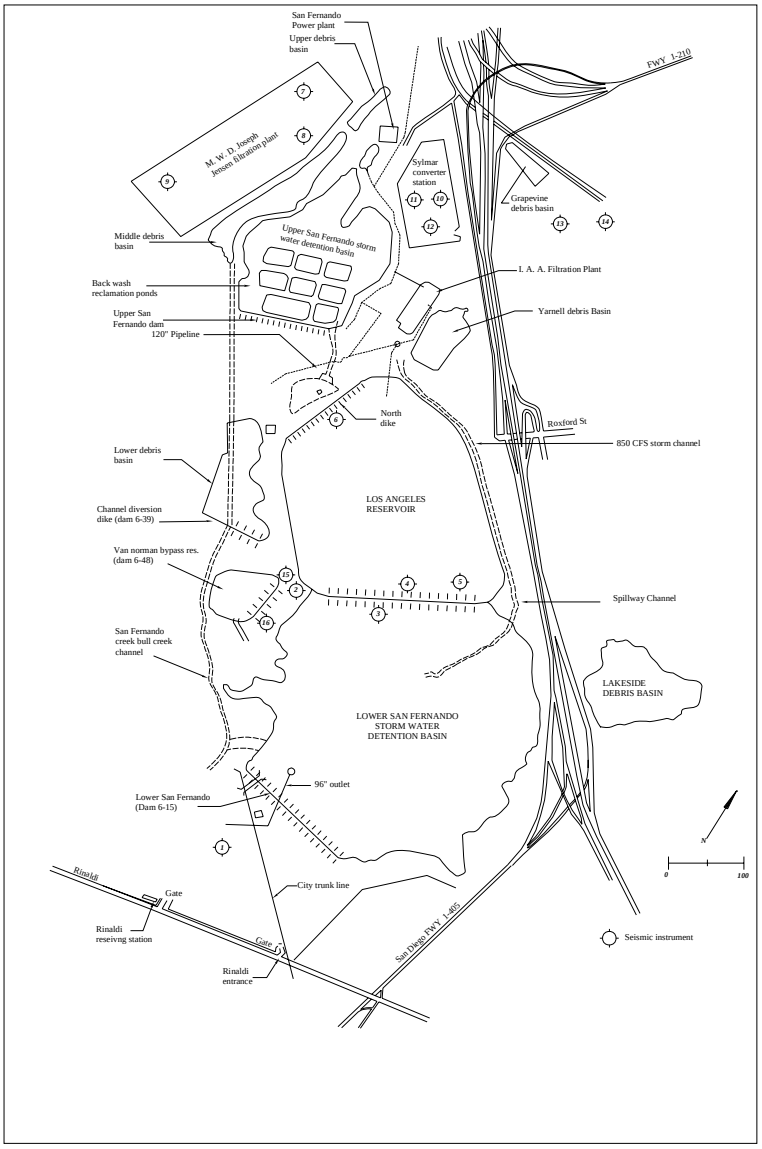

Figure 6. General view, main structures and location of strong motion recordings of Van Model response for irregular cycles (Modified from Davis and Bardet, 1996)

Lower San Fernando Dam

Although during the moment of the earthquake the basin was almost empty, the water level was usually found from 3 to 10 m below the crest of the dam. A typical cross section of the dam is presented in Figure 7. The upstream slope of the dam was reconstructed after the 1971 San Fernando Earthquake. The dam height is 40 m approximately, and was originally built using the hydraulic fill method. However, in several occasions it was added compacted fill to increase its storage capacity (Dawson, 2001). The material properties are summarized in Table 1. For the analysis, the core clay shear modulus was considered of 244600 kPa and for the other materials it was obtained as a function of the state of stresses according to the expression: $G = 22\ K_2\ (\sigma'_m)^{0.5}$, where σ'_m is the mean effective stress (in kPa). The values of K_2 are included in Table 1. The resistance to liquefaction was obtained using the corresponding blow counts, corrected by energy, obtained during SPT test. The seismic performance evaluation of the dam was conducted, considering the Northridge earthquake, 1995. CPT measurements taken after the earthquake indicate that the slide debris has an equivalent clean-sand blow count $(N_1)_{60}$ of 15 approximately.

Table 1. Material properties used in the analysis

Material	Unit weight (kN/m^3)	Friction Angle, ϕ, °	Cohesion, c kPa	K_2
Compacted fill	21.4	37	0	55
Compacted clay	21.4	37	10.3	55
Slide debris	17.0	37	0	43
Clay core	17.0	0	100.3	-
Alluvium	19.0	37	0	52

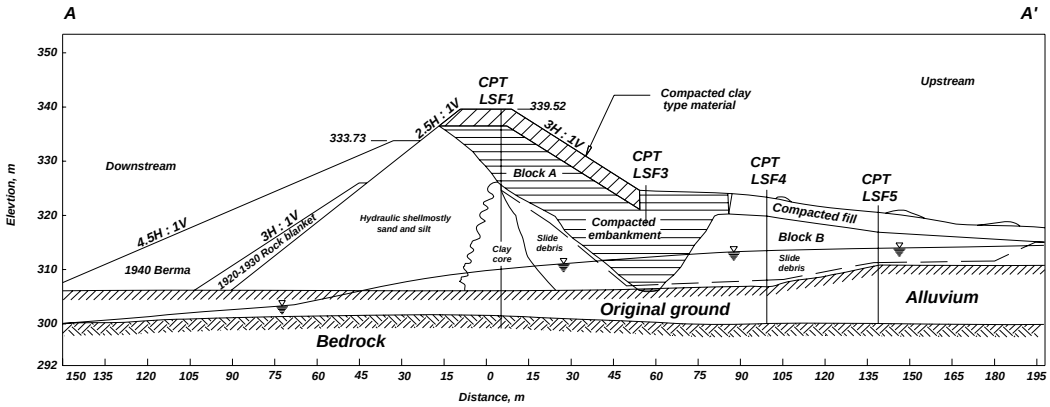

Figure 7. Cross section of repaired Lower San Fernando Dam (After Dawson et al., 2001)

Input ground motion

Figure 8 shows the acceleration time history utilized in the analysis, which corresponds to what was recorded in a seismological station located in the LA Dam west abutment record, and has a peak ground acceleration (PGA) of 0.43g, a fundamental period of 0.3 s and an approximate duration of the severe part of the earthquake of 15 s. Although a much higher PGA (0.86g) was recorded at Rinaldi Receiving station, located near the downstream toe of the lower San Fernando dam, apparently the record shows some site amplification due to its alluvial nature.

Analysis results

The finite difference model of the dam utilized in the dynamic analysis is shown in Figure 9. Figure 10 shows the pore pressure distributions before and after the earthquake, and Figure 11 presents contours of maximum vertical displacements. It can be seen that significant amounts of pore pressure developed after the earthquake, in the majority of the granular material located in the upstream face of the dam. A

comparison between the computed permanent horizontal displacement and field measurements are presented in Figure 12. It can be seen, that the model predicts favorably the measure displacements. The failure mechanism of the slopes can be observed in the plot of displacement vectors presented in Figure 13. It is clear that according to the simulation, when the soil liquefies, the failure does not occur as a rotation, but as a progressive movement in soil layers oriented preferentially horizontally, that is in agreement with the observation of cracks and general ground movement observed along the crest of the dam, during the damage survey conducted after the earthquake (Bardet y Davis, 1996a & b).

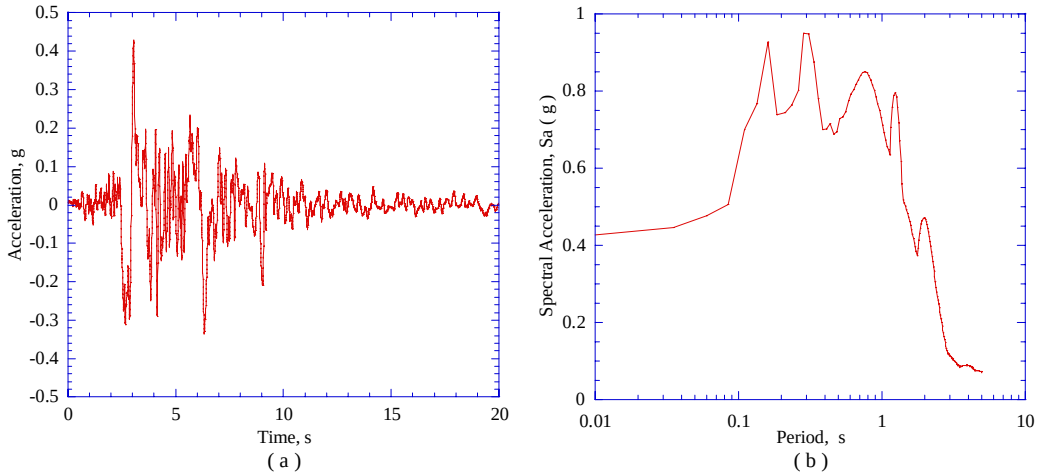

Figure 8. Input acceleration time history (a) and corresponding response spectrum (b)

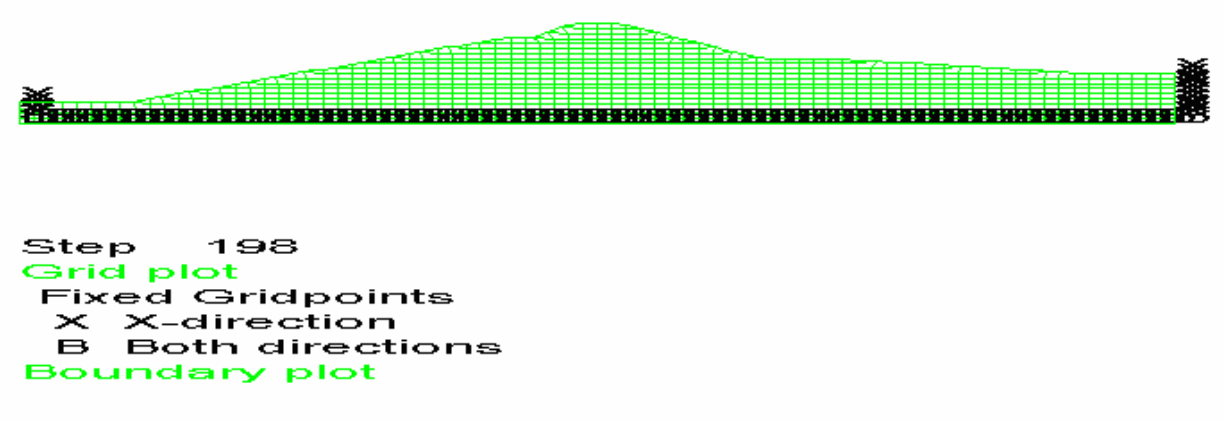

Figura 9. Finite difference model

Figure 14 shows the horizontal and vertical displacement computed at the tip of the upstream slope of the dam. It can be seen that the predicted displacement (0.15 m) is in good agreement with the measured response (0.16 m). Figure 15 shows the evolution of the pore pressure ratio, $r_u = \Delta u_g/\sigma_v'$, during the earthquake, for points A, B and C identified in Figure 10. It can be observed how r_u reaches a value of one at points A, B and C (r_u=1). The pore pressure increases importantly from the second 3.5, which as can be seen in the acceleration time history, corresponds to the beginning of the intense part of the earthquake. Furthermore, in t = 3.5 s approximately, it can be noticed a “pulse”, clearly identified in the velocity time histories computed in the aforementioned locations (Figure 16), that induced quite large shear stresses in the soil in a relatively short period of time, leading to a significant development of pore pressure. The corresponding histories of cyclic shear stresses for the three points are shown in Figure 17.

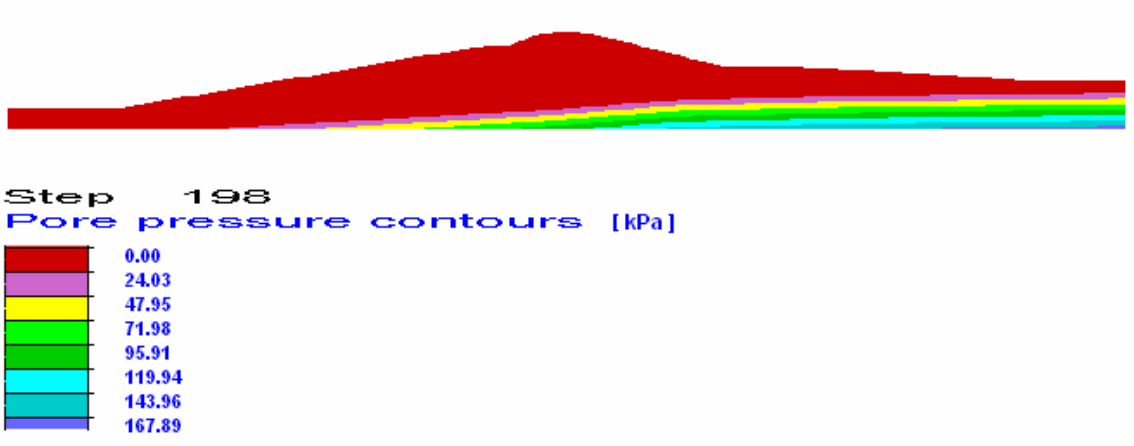

(a)

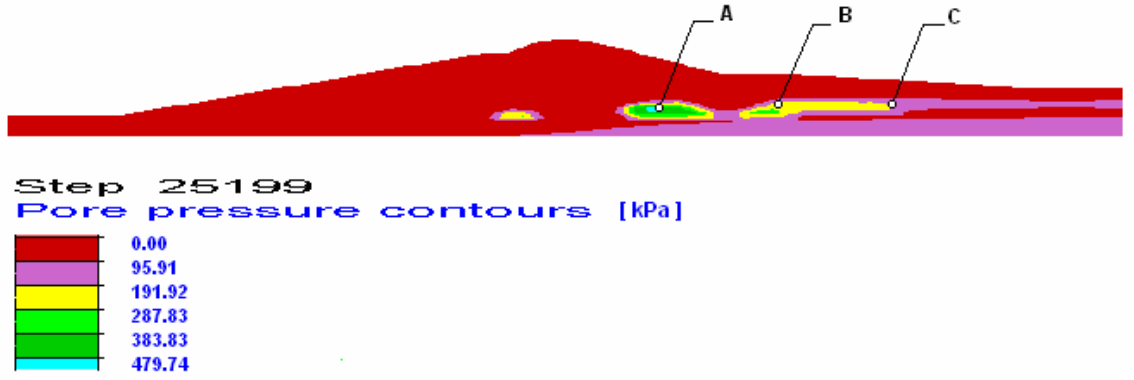

(b)

Figura 10. Pore pressure distribution (a) initial state and (b) final state

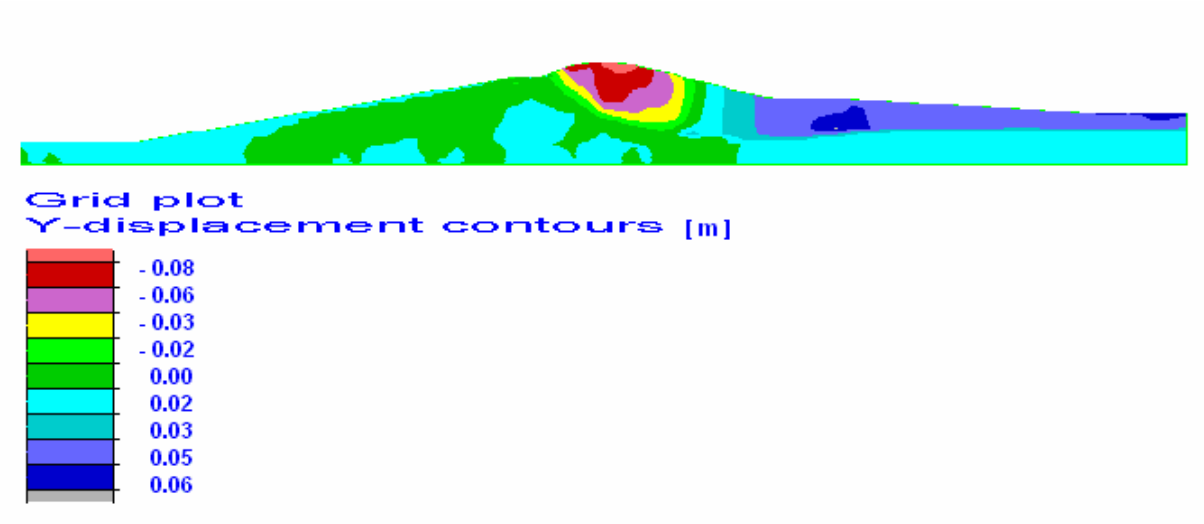

Figure 11. Vertical displacement distribution after the earthquake

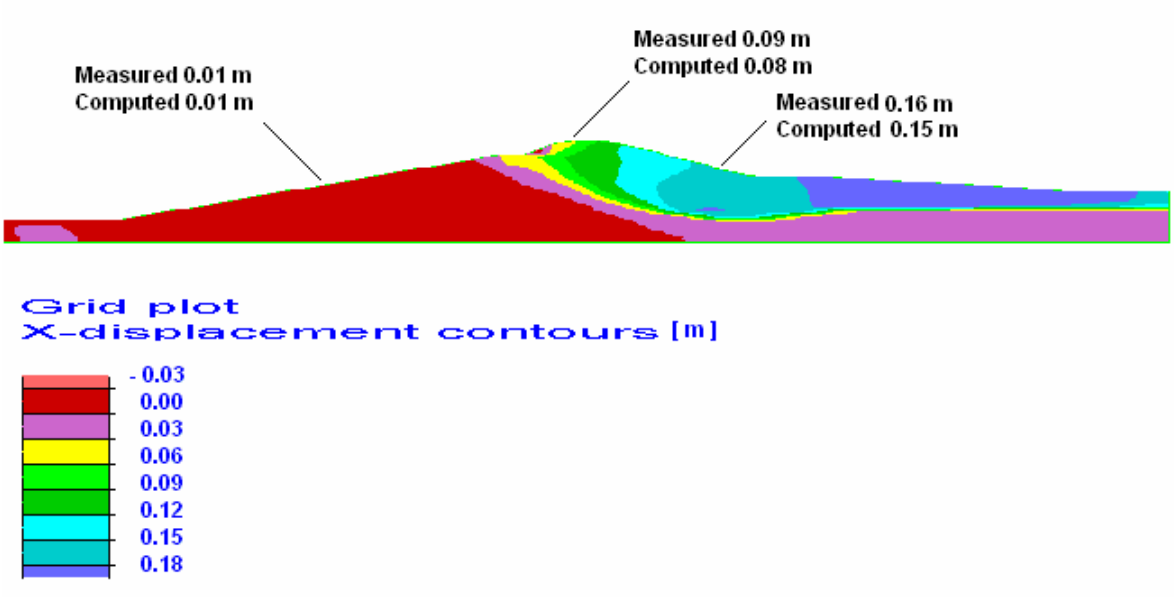

Figure 12. Contours of horizontal permanent displacements at the end of the earthquake

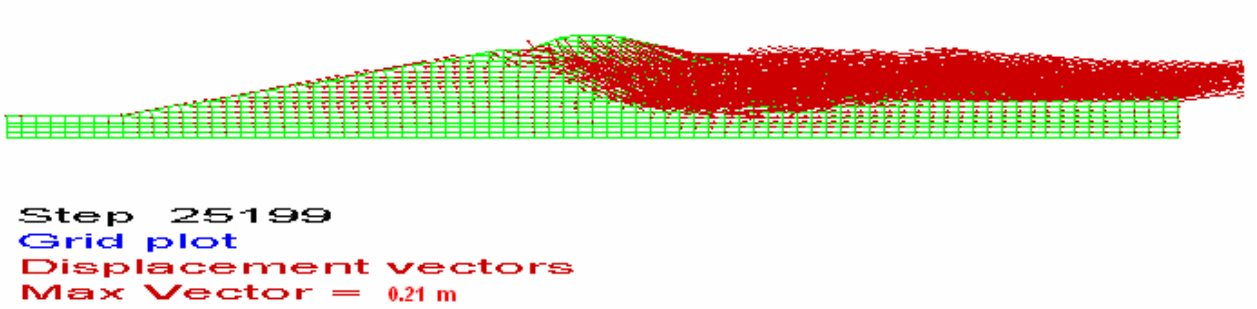

Figure 13. Displacement vectors after the earthquake

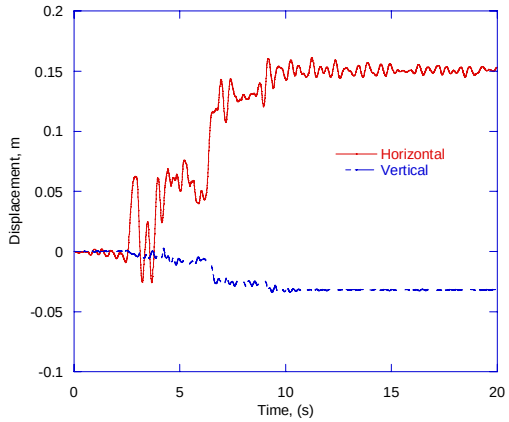

Figure 14. Horizontal and vertical displacements at the tip of the upstream slope

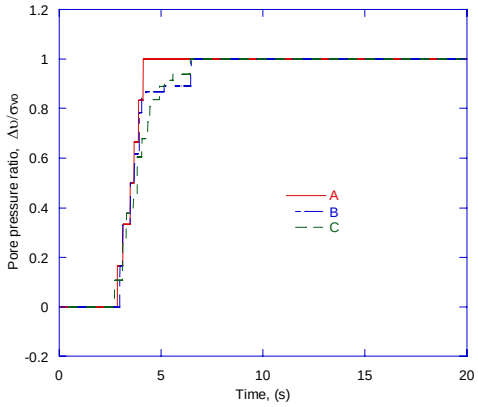

Figure 15. Pore pressure in points A, B and C of the dam

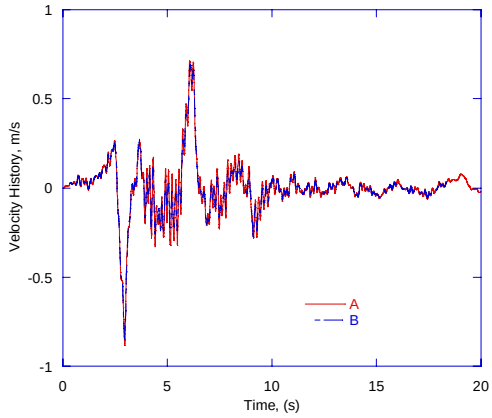

Figure 16. Velocity time histories in points A and B of the dam

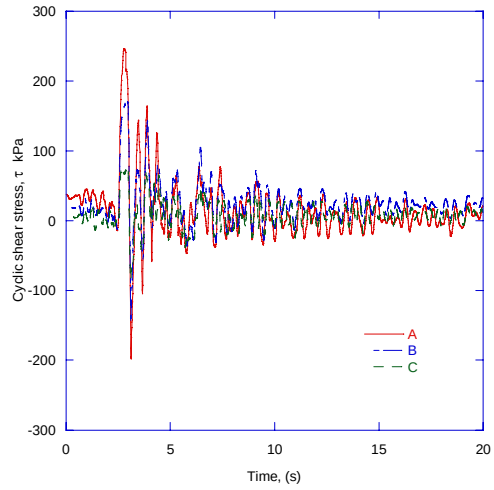

Figure 17. Cyclic shear stress histories in points A, B and C

CONCLUSIONS

Quantifying seismic risk zones around dams built with fine-grained saturated materials, requires conducting analyses that take into account the degree of internal distortion of the soil mass generated during the event, the drainage conditions, the localization of strength planes close to the surface of the soil, and the plastic yielding to depth. Simple models, such as the one presented in this paper, along with lagragian finite differences formulations allows to capture the overall response of the dam during

the earthquake both qualitatively as well as quantitatively, and are able to predict, the evolution of pore pressure, shear strength during the earthquake and the permanent displacement associated, as it was shown in the exampled discussed, of the lower San Fernando Dam.

REFERENCES

Bardet, J. P., and Davis, C. A., "Performance of San Fernando dams during the 1994 Northridge earthquake", J. Geotech. Eng. Div, ASCE, 122(7): 554-564, 1996a.

Bardet, J. P., and Davis, C. A., "Engineering observations of ground motion at the Van Norman Complex after the 1994 Northridge earthquake", Bull. Seism. Soc. Am., 86(1B):S333-S349, 1996b.

Castro, G., Poulos, S. J., and Leathers, F. D., "Re examination of slide of lower San Fernando Dam", J. Geotechnical Engrg., ASCE, 111(9), 1093-1107, 1985.

Davis, C.A., and Bardet, J. P., "Geotechnical observations at Van Norman Complex after the 1994 Northridge earthquake", 5th japan-US. Workshop on earthquake resistant design of lifeline facilites and countermeasures for soil liquefaction: Tech Rep. NCEER-94-0026, Nat Ctr. For Earthquake Engrg. Res., Buffalo, N. Y. 63-77, 1994.

Dawson E.M., Roth W.H., Nesarajah S., Bureau G., and Davis C.A., "A practice oriented pore pressure generation model", Proceedings, 2nd International FLAC Symposium, Lyon France, October, 2001.

Finn W. D. L., Lee K. W., and Martin G. R., "An Effective Stress Model for Liquefaction", Liquefaction Problems in Geotechnical Engineering. ASCE Annual Convention And Exposition. 169-198, 1976.

Morgenstern, N. R., Geotechnical aspects of environmental control, 1985.

Roth, W. H., and Cundall, P. A., "Nonlinear Dynamic Analysis of a Centrifuge Model Embankment", Proc. 3rd U.S. National Conference on Earthquake Engineering, august 23-28, Charleston, South Carolina, Vol. 1, 505-516, 1986.

Seed, H. B., Idriss, I. M. and Lee. K. L., "Analysis of Sheffield Dam failure", J. Soil Mechanics and Foundations Div., ASCE, 95(SM6), 1453-1490, 1969.

Seed, H. B. and Idriss, I. M., "Simplified procedure for evaluating soil liquefaction potential", J. Soil Mech. And Found. Div. ASCE, 97(SM9): 1249-1273, 1971.

Seed, H. B., Lee, K. L., Idriss, I. M. & Makdisi, F. I., "Analysis of the slides in the San Fernando dam during the earthquake of February 9, 1971", Rep. No. UCB/EERC-72/02, Univ. Of California Berkeley, 1973.

Seed, H. B., Martin, P. P., and Lysmer, J., "Pore-Water Pressure Changes During Soil Liquefaction", J. Geotech. Eng. Div., ASCE, 102(GT4): 323-346, 1976.

Seed H. B., "Evaluation of Soil Liquefaction Effects on Level Ground During Earthquakes", Liquefaction Problems in Geotechnical Engineering. ASCE Annual Convention and Exposition. 1-104, 1976.

Seed, H. B., "Soil liquefaction and cyclic mobility evaluation for level ground during earthquakes", J. Geotech. Eng. Div., ASCE, 105(GT2): 201-255, 1979.

Seed, H.B., Seed, R.B., Harder, L. F. & Jong, H. L., "Reevaluation of the slide in the Lower San Fernando Dam in the 1971". Rep. No. UCB/EERC-88/04, Univ. of California Berkeley, 1989.

Seed, H.B. and Harder, L. F., "SPT-Based analysis of Cyclic Pore Pressure Generation and Undrained Residual Strength", in., Proceedings, H. Bolton Seed Memorial Symposium, J. M. Duncan (ed.), University of California, Berkeley, Vol. 2. 351-376. 1990.

Stark, T. D. and Mesri, G., "Undrained Shear strength of Sands for Stability Analysis", J. of Geotech. Eng., ASCE, 118(11): 1727-1747, 1992.

Youd, T. L. and Idriss, I. M., "Liquefaction resistance of soils: summary report from the 1996 NCEER and 1998 NCEER/NSF workshops on evaluation of liquefaction resistance of soils", J. Geotech. And Geoenvir. Eng., ASCE, 127(4): 297-313, 2001.

Wang Zhi-Liang, Makdisi, Faiz I., and John Egan, "Practical applications of a nonlinear approach to analysis of earthquake-induced liquefaction and deformation of earth structures", In Soil Dyn. And Earthquake Eng. (26): 231-252, 2006.